Coexistence of magnetic order and Kondo effect in the Kondo-Heisenberg model

B. H. Bernhard[1,*] and C. Lacroix[2]

[1]*Departamento de Física, Universidade do Estado de Santa Catarina, 89.219-710 Joinville, SC, Brazil*

[2]*Institut Néel, Université Grenoble Alpes et CNRS, F38042 Grenoble, France*

(Received 23 December 2014; published 1 September 2015)

The Kondo lattice model is investigated through a fermionic mean-field approximation. The obtained phase diagram, including the pure ferromagnetic (FM), antiferromagnetic (AF), Kondo (K), and mixed phases, is in good agreement with previous studies. Calculations on the simple cubic and square lattices confirm a robust coexistence of ferromagnetism and Kondo effect (FM + K), sustained by a partial Kondo screening, which leads to the concept of a spin selective Kondo insulator. We have also obtained a coexistence of antiferromagnetism and Kondo effect (AF + K), which requires the intervenience of a next-nearest-neighbor hopping t' and a Heisenberg exchange J_{ij}. The effect of temperature and pressure is described by the behavior of the order parameters. The corresponding Néel temperature T_N and Kondo temperature T_K are plotted in the form of a Doniach diagram. The presence of the intermediate mixed phases is fundamental to determine the order of the magnetic phase transitions as one approaches the quantum critical point.

DOI: 10.1103/PhysRevB.92.094401 PACS number(s): 75.20.Hr, 71.10.Fd

I. INTRODUCTION

The magnetic properties of heavy-fermion materials are mainly determined from the competition between the Kondo effect and magnetic order, usually described within the framework of the Anderson lattice or Kondo lattice Hamiltonians [1,2]. Despite the cumulative theoretical work on these models, through different many-body techniques, several points remain to be further explored, implying a generalization of the standard Doniach diagram in multiple aspects. In antiferromagnetic materials such as $YbRh_2Si_2$ and $CeCu_2Si_2$, different types of magnetic transitions can be found, which may involve a reconstruction of the Fermi surface in the neighborhood of the quantum critical point (QCP) [3–5]. In the case of ferromagnetic materials, a long-standing challenge concerns the attainability of a ferromagnetic QCP [6–11]. Recently, the need of a global phase diagram, which includes the interplay of frustration and Kondo effect [12,13], has been emphasized. Furthermore, new phases have been identified in these systems, e.g., with charge order [14–16] or partial Kondo screening, where Kondo screened sites coexist with magnetic sites [17,18].

In this context, the mean-field pseudofermion approach remains a valuable tool, as it provides a unifying picture for the various heavy-fermion compounds, with the ability of unveiling new phases, as recently brought into evidence. Nevertheless, a variety of such approximations can be found in the literature, and they may not be *a priori* equivalent. Some of the concerned papers considered the interplay of the Kondo effect with short-range magnetic correlations [19–21]. The Lifshitz transitions reported in Refs. [22,23] refer to this case. Long-range magnetic order has been included within the fermionic approach in Refs. [24–33], and the effect of a magnetic field has been considered in Refs. [34,35]. In Ref. [36], a dynamical mean-field theory study revealed the existence of a spin-selective Kondo insulator (SSKI), where the Fermi level is located at the gap for one spin direction only. This state corresponds to the mixed ferromagnetism and Kondo effect (FM + K) state with a plateau in the total magnetization, as reported in Refs. [26–28]. In Refs. [32,33], a rich phase diagram has been obtained for the frustrated Shastry-Sutherland lattice.

We propose here an alternative version of the method which is adequate to describe the competition between magnetic order and Kondo effect, including their possible coexistence. We argue that the intrinsic ambiguity in defining the particular decoupling of the interaction terms appearing in the Kondo lattice model can be circumvented by an appropriate choice of the starting Hamiltonian and the order parameters.

For concreteness, we will focus on a square lattice. This choice has been motivated by the possibility of a direct comparison with the literature, and also by its connection to the Shastry-Sutherland lattice, considered in Ref. [32]. We also discuss some results obtained for a constant density of states and for a simple cubic lattice. The idea is to analyze and test the performance of the fermionic mean-field approach as a reliable approximation to the Kondo lattice and related models.

The present results confirm and complement some previous related studies, reinforcing their significance. They clarify the evolution of the phase diagram as a function of the relevant parameters, including the effect of the Kondo interaction J_K, the intersite exchange J_{ij}, the hoppings t_{ij}, the electronic concentration n, and the temperature T.

In the next section, we introduce the fermionic mean-field approach for the Kondo-Heisenberg Hamiltonian. In Sec. III, we present some selected results describing the phase diagram of the model on a square lattice, and connect the present work with previous related studies. In Sec. IV, we complement the discussion and present a summary of the conclusions.

II. MODEL AND APPROXIMATION

A. The fermionic Hamiltonian

The Kondo lattice and Anderson lattice Hamiltonians, without losing their respective identities as independent physical

*benhur.bernhard@udesc.br

models, may be related to each other in the appropriate limits, as discussed, e.g., in Ref. [37]. The correspondence between these models has been established in Ref. [2], based on the Schrieffer-Wolff transformation [38]. The interacting part of the Hamiltonian generated by this canonical transformation can be written as a sum of terms

$$\mathcal{H}_K = \mathcal{H}'_K + \mathcal{H}_{cf} + \mathcal{H}_{ch}, \tag{1}$$

where

$$\mathcal{H}'_K = J_K \sum_i \mathbf{S}_i \cdot \mathbf{s}_i, \tag{2}$$

$$\mathcal{H}_{cf} = -J_K/4 \sum_{i\sigma\sigma'} n^f_{i\sigma'} n^c_{i\sigma}, \tag{3}$$

$$\mathcal{H}_{ch} = -J_K/4 \sum_{i\sigma} (c^\dagger_{i\bar{\sigma}} c^\dagger_{i\sigma} f_{i\sigma} f_{i\bar{\sigma}} + \text{H.c.}). \tag{4}$$

The term $\mathcal{H}'_K$ describes a local antiferromagnetic exchange interaction (with $J_K > 0$) between localized spins $\mathbf{S}_i$ and conduction electron spins $\mathbf{s}_i$.

The fermionic representation for the localized spins with $S = 1/2$ introduces pseudofermion or spinon operators $f^\dagger_{i\sigma}$ and $f_{i\sigma}$ (reminiscent from the f-electron orbital in the original Anderson lattice model):

$$S^z_i = \tfrac{1}{2}\left(n^f_{i\uparrow} - n^f_{i\downarrow}\right), \tag{5}$$

$$S^\sigma_i = S^x_i + i z_\sigma S^y_i = f^\dagger_{i\sigma} f_{i\bar{\sigma}}, \tag{6}$$

where $n^f_{i\sigma} = f^\dagger_{i\sigma} f_{i\sigma}$ is the pseudofermion number operator, and $z_\uparrow = +1$, $z_\downarrow = -1$. Similar expressions can be used for the conduction electron spins $\mathbf{s}_i$ in terms of operators $c^\dagger_{i\sigma}$ and $c_{j\sigma}$.

The scalar product of spin operators in Eq. (2) can be factorized as

$$\mathbf{S}_i \cdot \mathbf{s}_i = \frac{1}{2} \sum_\sigma f^\dagger_{i\bar{\sigma}} f_{i\sigma} c^\dagger_{i\sigma} c_{i\bar{\sigma}} + \frac{1}{4} \sum_{\sigma\sigma'} z_\sigma z_{\sigma'} f^\dagger_{i\sigma} f_{i\sigma} c^\dagger_{i\sigma'} c_{i\sigma'}. \tag{7}$$

Before proceeding to any decoupling of the products of four operators appearing in Eq. (7), we adopt an alternative expression for the Hamiltonian defined by Eqs. (1)–(4) in the form

$$\mathcal{H}_K = -J_K \sum_{i\sigma} \lambda_{i\bar{\sigma}} \lambda_{i\sigma} - J_K/2 \sum_{i\sigma} n^f_{i\bar{\sigma}} n^c_{i\sigma}, \tag{8}$$

where we introduce the Hermitian operator

$$\lambda_{i\sigma} = 1/2 (f^\dagger_{i\sigma} c_{i\sigma} + c^\dagger_{i\sigma} f_{i\sigma}). \tag{9}$$

Heisenberg exchange interactions $\sum_i J_{ij} \mathbf{S}_i \cdot \mathbf{S}_j$ can also be included in the model to account for the interactions between localized spins $\mathbf{S}_i$:

$$\mathcal{H}_H = -1/2 \sum_{ij\sigma} J_{ij} \tilde{\gamma}^{\bar{\sigma}}_{ij} \tilde{\gamma}^\sigma_{ij} - 1/4 \sum_{ij\sigma} J_{ij} n^f_{i\bar{\sigma}} n^f_{j\sigma}, \tag{10}$$

where

$$\tilde{\gamma}^\sigma_{ij} = 1/2 (f^\dagger_{i\sigma} f_{j\sigma} + f^\dagger_{j\sigma} f_{i\sigma}). \tag{11}$$

This term incorporates the Ruderman-Kittel-Kasuya-Yosida interaction induced by the Kondo exchange coupling J_K (see, e.g., Refs. [16,37]). By second-order perturbation theory, an effective coupling $J_{ij} \sim J_K^2$ is found in the pure Kondo lattice, so that magnetic phases are present even in this case. With the explicit inclusion of this Heisenberg term, J_{ij} will be considered here as an independent parameter, as in Ref. [32].

The model is thus described by the complete Hamiltonian

$$\mathcal{H} = \mathcal{H}_t + \mathcal{H}_K + \mathcal{H}_H, \tag{12}$$

where

$$\mathcal{H}_t = -\sum_{ij\sigma} t_{ij} c^\dagger_{i\sigma} c_{j\sigma} \tag{13}$$

represents the conduction electron band.

The Hamiltonian expressed by Eq. (12) [with its terms defined in Eqs. (8), (10), and (13)] constitutes by itself a third independent model, in addition to the Kondo lattice and Anderson lattice Hamiltonians. From the way it was derived, it is conceptually located in between these two traditional models, so that it should lead presumably to the same physics as the Kondo lattice, in the limit of validity of the Schrieffer-Wolff transformation.

B. Mean-field approximation

The products of operators in Eqs. (8) and (10) can be treated following a standard mean-field approximation

$$\lambda_{i\bar{\sigma}} \lambda_{i\sigma} \approx \langle \lambda_{i\bar{\sigma}} \rangle \lambda_{i\sigma} + \langle \lambda_{i\sigma} \rangle \lambda_{i\bar{\sigma}} - \langle \lambda_{i\bar{\sigma}} \rangle \langle \lambda_{i\sigma} \rangle, \tag{14}$$

$$\tilde{\gamma}^{\bar{\sigma}}_{ij} \tilde{\gamma}^\sigma_{ij} \approx \langle \tilde{\gamma}^{\bar{\sigma}}_{ij} \rangle \tilde{\gamma}^\sigma_{ij} + \langle \tilde{\gamma}^\sigma_{ij} \rangle \tilde{\gamma}^{\bar{\sigma}}_{ij} - \langle \tilde{\gamma}^{\bar{\sigma}}_{ij} \rangle \langle \tilde{\gamma}^\sigma_{ij} \rangle, \tag{15}$$

$$n^f_{i\bar{\sigma}} n^c_{i\sigma} \approx \langle n^f_{i\bar{\sigma}} \rangle n^c_{i\sigma} + \langle n^c_{i\sigma} \rangle n^f_{i\bar{\sigma}} - \langle n^f_{i\bar{\sigma}} \rangle \langle n^c_{i\sigma} \rangle, \tag{16}$$

$$n^f_{i\bar{\sigma}} n^f_{j\sigma} \approx \langle n^f_{i\bar{\sigma}} \rangle n^f_{j\sigma} + \langle n^f_{j\sigma} \rangle n^f_{i\bar{\sigma}} - \langle n^f_{i\bar{\sigma}} \rangle \langle n^f_{j\sigma} \rangle. \tag{17}$$

We obtain an effective fermionic Hamiltonian describing hybridized, uncorrelated bands

$$\mathcal{H}' = \mathcal{H}_t + \mathcal{H}_{\tilde{t}} + \mathcal{H}_{\tilde{V}} + \mathcal{H}_f + \mathcal{H}_h, \tag{18}$$

where

$$\mathcal{H}_{\tilde{t}} = -\sum_{ij\sigma} \tilde{t}^\sigma_{ij} f^\dagger_{i\sigma} f_{j\sigma}, \tag{19}$$

$$\mathcal{H}_{\tilde{V}} = -\sum_{i\sigma} \tilde{V}_{i\sigma} (f^\dagger_{i\sigma} c_{i\sigma} + c^\dagger_{i\sigma} f_{i\sigma}), \tag{20}$$

$$\mathcal{H}_h = \sum_{i\sigma} z_\sigma \left(h^f_i + \tilde{h}_i\right) n^f_{i\sigma} + \sum_{i\sigma} z_\sigma h^c_i n^c_{i\sigma}, \tag{21}$$

and

$$\mathcal{H}_f = E_f \sum_{i\sigma} n^f_{i\sigma}. \tag{22}$$

The effective parameters depend on the self-consistent mean-field parameters: $\tilde{t}^\sigma_{ij} = J_{ij} \langle \tilde{\gamma}^{\bar{\sigma}}_{ij} \rangle$ and $\tilde{V}_{i\sigma} = J_K \langle \lambda_{i\bar{\sigma}} \rangle$. Magnetic long-range order is related to the molecular fields $h^f_i = \frac{1}{2} J_K \langle s^z_i \rangle$ and $h^c_i = \frac{1}{2} J_K \langle S^z_i \rangle$, which imply a magnetic coupling between local and itinerant moments, and $\tilde{h}_i = 1/2 \sum_j J_{ij} \langle S^z_j \rangle$, which couples directly the localized spins at neighboring sites.

The energy E_f is a Lagrange multiplier introduced in Eq. (22) in order to fix the f electron number $\langle n_f \rangle = \sum_\sigma \langle n_{i\sigma}^f \rangle = 1$. The chemical potential μ is fixed from the constraint $\sum_\sigma \langle n_{i\sigma}^c \rangle = n$, where n is the conduction electron concentration.

The transformation from the Anderson to the Kondo lattice Hamiltonian introduces a constraint on the f-electron concentration, which may be imposed explicitly as $n_f = 1$ (by projecting out the states with $n_f \neq 1$), or on the average as $\langle n_f \rangle = 1$. The former would imply a vanishing value of $\langle \lambda \rangle$. On the other hand, most pseudofermion approaches (including the present one) adopt the latter choice of the constraint, which allows a finite value of $\langle \lambda \rangle$. Within the mean-field decoupling, $\langle \lambda \rangle$ assumes the role of an order parameter associated with the Kondo "phase."

In a similar way, the average $\langle \tilde{\gamma} \rangle$ describes the correlation between magnetic moments at neighboring sites, as discussed in Ref. [21]. It allows a correct treatment of valence bond solid and spin-liquid (resonating-valence-bond-type) states [32]. Here the pure magnetic phases (without coexistence) consist of quite trivial magnetic solutions (of the complete Hamiltonian) with both $\langle \lambda \rangle = 0$ and $\langle \tilde{\gamma} \rangle = 0$. These mean-field parameters acquire a new interpretation after the introduction of the effective Hamiltonian in Eq. (18). The parameters E_f and $\tilde{V}$ become clearly distinct from the corresponding parameters E_f and V in the original Anderson model.

The internal energy per site corresponding to the original Hamiltonian $\mathcal{H}$ in Eq. (12) can be expressed as

$$E = -\sum_{j\sigma} t_{ij}^\sigma \langle \gamma_{ij}^\sigma \rangle - \frac{1}{2} \sum_{j\sigma} \tilde{t}_{ij}^\sigma \langle \tilde{\gamma}_{ij}^\sigma \rangle - \sum_\sigma \tilde{V}_{i\sigma} \langle \lambda_{i\sigma} \rangle + \tilde{h}_i \langle S_i^z \rangle + J_K \langle S_i^z \rangle \langle s_i^z \rangle, \quad (23)$$

where $\gamma_{ij}^\sigma = 1/2(c_{i\sigma}^\dagger c_{j\sigma} + c_{j\sigma}^\dagger c_{i\sigma})$.

The phase diagram is determined by the competition among the multiple phases described by the self-consistent parameters $\langle \lambda_{i\sigma} \rangle$ and $\langle S_i^z \rangle$. They include the pure ferromagnetic (FM) and antiferromagnetic (AF) phases, in absence of Kondo effect, with $\langle \lambda_{i\sigma} \rangle = 0$ and $\langle S_i^z \rangle, \langle s_i^z \rangle \neq 0$; the pure Kondo (K) phase in absence of magnetic order, with $\langle \lambda_{i\sigma} \rangle, \langle \tilde{\gamma}_{ij}^\sigma \rangle \neq 0$ and $\langle S_i^z \rangle = 0$; and also the mixed phases with coexistence, where all averages are different from zero. In the case of coexistence, the numerical solution interpolates between the adjacent pure phases. Differently from previous approaches [30,33], the method does not require any control parameter x, because each term appearing in Eqs. (8) and (10) evokes only one of the allowed order parameters.

III. RESULTS

A. The pure Kondo lattice case (J,$t' = 0$)

For the sake of comparison with the literature, we have applied the present decoupling to the case of a rectangular density of states, adopted in most of the related treatments [2,19,21,24–28,31,39]. The corresponding results will not be shown explicitly, as additional figures, in this section, but it is important to comment on them, stressing the coincidences and eventual divergences.

The results obtained (if one restricts to the pure phases FM, AF, and K) reproduce quantitatively the ground-state phase diagram $J_K \times n$ of the Kondo lattice model shown in Fig. 4 from Ref. [2]. Such coincidence is far from obvious, because the phase boundaries depend strongly on the particular way the two terms in the right-hand side of Eq. (7) are decoupled. This agreement establishes a correspondence between the present version of the fermionic mean-field approach, and the method adopted in Ref. [2], which relies on a functional integration approach based on a Hubbard-Stratanovitch transformation.

A similar diagram has been obtained in Fig. 3 of Ref. [39] by the Gutzwiller variational method. It is worth remarking that, in this reference, $n = (n_c + 1)/2$, where n_c is the electronic concentration, so that the FM/AF interface at $n = 0.82$ corresponds to $n_c = 0.64$, which coincides with Ref. [2]. Thus, a quantitative difference between the two diagrams is evident only in the vertical axis, where the magnetic region is reduced by a factor about $1/2$ in Ref. [39].

We have also obtained a coexistence of ferromagnetic order and Kondo effect (FM + K) in a region between the pure K and FM phases, where our results are in good agreement with those reported in Refs. [26–28]. Our calculated diagram including the phase FM + K is very similar to Fig. 2(a) from Ref. [27]. Again, this coincidence indicates an equivalence between the two calculations, even though the decoupling approximations are justified in a different way. However, the mentioned figure from Ref. [27] does not show the location of the AF phase, which should be present for $n > 0.64$, as discussed above. We have also verified that the pure AF phase is stable against the FM + K phase (when both solutions are present). We have not found any region of coexistence AF + K for $J = 0$, in contrast to Ref. [31], where it has been detected in a narrow region between the AF and K phases.

The results presented below correspond to calculations performed on a square lattice with nearest-neighbor and next-nearest-neighbor hoppings t and t', respectively. We also considered the effect of a nearest-neighbor exchange $J_{ij} = J$. As a first step to construct the phase diagram, we have considered the pure K, FM, and AF self-consistent solutions. Equation (23) is then used to determine the stable phase for a given set of parameters: t, t', J_K, J, and the conduction electrons concentration n.

We apply the Green's function method to the effective Hamiltonian $\mathcal{H}'$, as described in Ref. [32]. For the ferromagnetic and nonmagnetic phases, the system of equations is solved by direct spatial Fourier transformation on the square lattice, assuming a homogeneous solution with site independent averages. For the antiferromagnetic phase, a two-site basis has to be considered, where translational invariance is assumed on the two sublattices. The solution is formally similar to the case of the Shastry-Sutherland lattice in Ref. [32], but with matrices of size 2×2, and including all diagonal hopping terms. The thermal averages are computed in the standard way, by integrating the self-consistently calculated densities of states multiplied by the Fermi distribution function [26,40].

Figure 1 illustrates the phase diagram of the Kondo lattice at zero temperature with $J = 0$ and $t' = 0$. The K phase dominates for sufficiently large values of J_K, which depends on the electron concentration n. For small J_K, the AF phase appears around half-filling for $n > 0.586$, and the FM phase

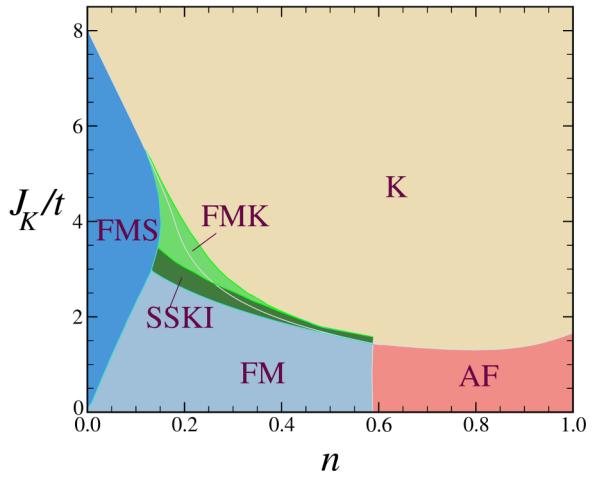

FIG. 1. (Color online) Ground-state phase diagram of the KLM on a square lattice for $t' = 0$ and $J = 0$, showing the mixed phases SSKI and FMK.

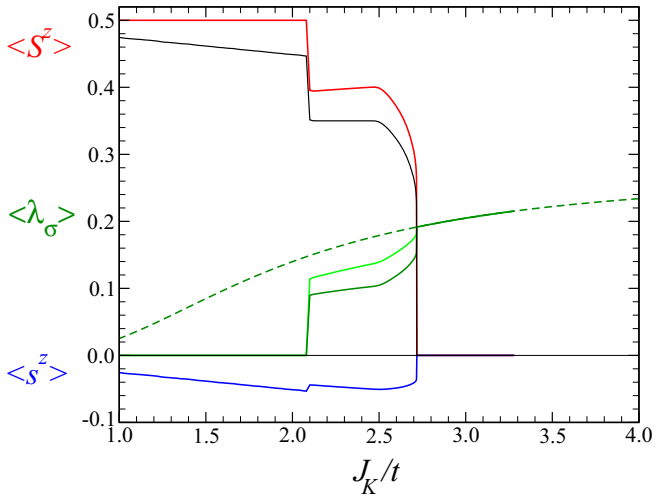

FIG. 2. (Color online) Magnetizations $\langle S_i^z \rangle$ (red) and $\langle s_i^z \rangle$ (blue), and the averages $\langle \lambda_{i\sigma} \rangle$ (green) as a function of J_K for $n = 0.3$, $t' = 0$, and $J = 0$ in the low-temperature limit. The dashed line corresponds to the value of $\langle \lambda_{i\sigma} \rangle$ in the pure K phase. The black line is the total magnetization $\langle S_i^z \rangle + \langle s_i^z \rangle$.

dominates at lower concentrations. The diagram is symmetric with respect to $n = 1$. The saturated FM solution (in which $\langle s_i^z \rangle = -n/2$) is identified as FMS. Nearby the underlying FM/K boundary (marked by a thin line) one can identify an intermediate region of coexistence of ferromagnetism and Kondo effect (FM + K).

Two regions, named SSKI and FMK, can be distinguished within the mixed FM + K phase. The lower J_K region corresponds to a SSKI state, characterized by the formation of a partial Kondo singlet combining all minority-spin conduction electrons ($\langle n_\uparrow^c \rangle$) with an equivalent number of majority-spin conduction electrons and f electrons of both spins [36]. The remaining majoritary-spin f and c electrons are antiferromagnetically coupled at each site, forming a ferromagnetic state. The corresponding commensurability condition $\langle n_\uparrow^c \rangle = \langle n_\downarrow^f \rangle$ emerges spontaneously in this region, associated to a plateau in the total magnetization $\langle S_i^z \rangle + \langle s_i^z \rangle = (1 - n)/2$.

The evolution of the order parameters through the mixed phase region is shown in Fig. 2. The transition from the FM phase to the SSKI phase is marked by discontinuities in the averages $\langle \lambda_{i\sigma} \rangle$, $\langle S_i^z \rangle$, and $\langle s_i^z \rangle$ (around $J_K/t = 2.1$). The total magnetization is illustrated by the black line, which exhibits a horizontal plateau (for $2.1 < J_K/t < 2.5$) in the SSKI state. By further increasing J_K/t, the system enters a competing (FMK) region, where the Kondo effect gradually reduces the magnetizations $\langle S_i^z \rangle$ and $\langle s_i^z \rangle$, leading eventually to a sharp transition to the nonmagnetic K phase (around $J_K/t = 2.7$). The dashed line shows the behavior of $\langle \lambda_{i\sigma} \rangle$ in the pure K phase in absence of magnetic order, when it would be nonzero down to $J_K = 0$. The Kondo breakdown is characterized by the vanishing of $\langle \lambda_{i\sigma} \rangle$ at $J_K = 2.2t$ when magnetic order is allowed.

The phase diagram depicted in Fig. 1 can be compared with the phase diagram shown in Fig. 9 of Ref. [39] for the square lattice. Again, we observe a perfect agreement in the position of the boundary FM/AF about $n_c = 0.58$. After transforming the values expressed in the vertical axis, the magnetic region is reduced by the same factor 1/2 when compared to our method, as observed above in the case of a constant density of states. It is evident, from both methods, that the lattice geometry affects the details of the phase diagram. Therefore, when we include the mixed phases, we are generalizing the previous diagrams reported in Refs. [27,39] in multiple aspects.

Figure 3 shows the densities of states of spin-up and spin-down electrons in the presence of the magnetization plateau. The arrow indicates the Fermi level position, which clearly lies inside a gap in the minority (up) spin band, while the majority (down) spin band is conducting.

We have also evaluated the corresponding curves of the Curie temperature T_C and the Kondo temperature T_K as a function of J_K/t, which lead to a ferromagnetic Doniach diagram, qualitatively similar to the phase diagram obtained in Ref. [26] assuming a constant density of states.

B. The Kondo-Heisenberg lattice (with $J, t' \neq 0$)

As the antiferromagnetic exchange coupling J is turned on, the AF phase grows into the FM region, which eventually is shifted into the K region, becoming unstable. The evolution of the pure phases FM, AF, and K as a function of J and t' is illustrated in Fig. 4. We observe that the value $J = 0.5t$ is sufficiently high to entirely suppress the FM phase in Fig. 4(b). In the presence of t', the diagram becomes asymmetric with respect to half-filling, as shown in panel 4(c). Figure 4(d) illustrates the opposite case with a ferromagnetic coupling $J < 0$, where the phase diagram yields a sequence of transitions FM-AF-K as a function of J_K (for $0.82 < n < 1.00$), which corresponds to the observed behavior, e.g., in $CeRu_2Ge_2$ [7] and $CeAgSb_2$ [8] under pressure.

The phase boundaries are defined from the intersections of the energy curves for the competing solutions. This is shown in Fig. 5 for $n = 0.8$, $t' = 0.8t$, and $J = 0.5t$, as the crossing of the K and AF energy curves. Figure 5 also shows the solution AF + K with coexistence of antiferromagnetic long-range order and Kondo effect, which turns out to be

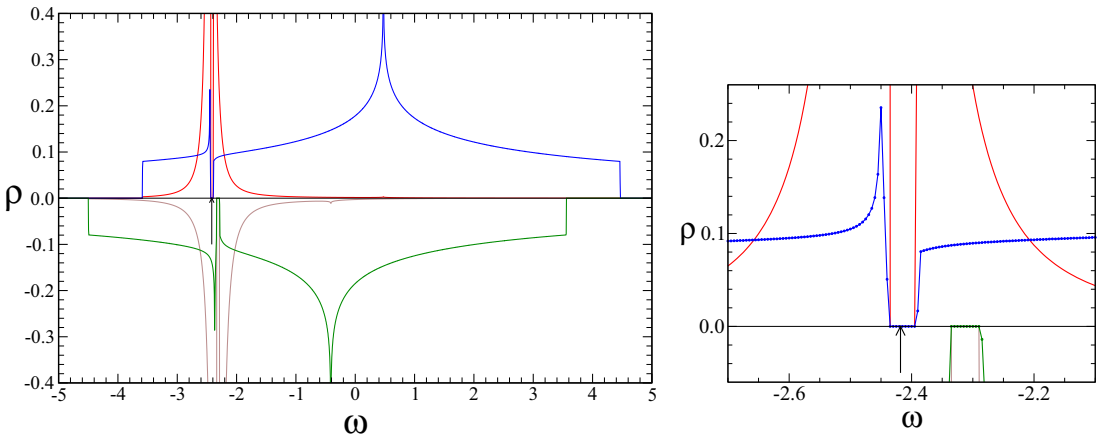

FIG. 3. (Color online) Densities of states for spin-up (top) and spin-down (bottom) f and c electrons for $J_K = 2.3t$ and $n = 0.3$, in the SSKI phase. The inset amplifies the region around the Fermi level.

favored in the neighborhood of the AF/K boundary. The energy curve of the AF + K phase interpolates smoothly between the pure K and AF curves.

The boundaries of the region AF + K can be determined from the order parameters. They are plotted in Fig. 6 as a function of J_K/t for a fixed value of n. The curves show how the magnetic moments are reduced by the Kondo effect. The transition from the AF + K phase to the AF phase, as J_K decreases, is continuous, with the order parameters $\langle\lambda_{i\sigma}\rangle$ decreasing smoothly to zero. Analogously, the transition from the AF + K phase to the K phase, as J_K increases, is marked by the vanishing of the magnetization curves at a given value J_{Kc}. The effect of temperature T is also illustrated. As T increases, the value of J_{Kc} shifts downwards, while the width of the AF + K region decreases. The transition AF + K/K becomes sharper as the temperature is further reduced below $T = 0.01t$. The dashed line indicates the variation of $\langle\lambda_{i\sigma}\rangle$ in the pure K phase. As discussed above with respect to Fig. 2, the presence of magnetic order anticipates the vanishing of these spin dependent order parameters, which evolve gradually within the mixed phase.

Comparing to the FM case described above, a noticeable difference concerns the respective transitions from the pure magnetic phase to the mixed phase, which was discontinuous in the FM case (associated with the appearance of the magnetization plateau in the SSKI phase), but is found to be continuous in the AF case. Following the analysis of the case $t = 0$, $t' \neq 0$ in Ref. [29], one can infer that the same mechanism leading to the SSKI phase is present in each sublattice, contributing to sustain the coexistence AF + K, although no corresponding SSKI phase can be distinguished for $t \neq 0$ as in the ferromagnetic case.

Figure 7 shows the evolution of the Fermi surface (which is holelike) from the pure AF phase to the mixed AF + K phase, changing from a squarelike shape to a circle as it approaches the K phase. For $J_K = 3.50t$, the f electrons are localized and completely decoupled from the conduction electrons, but for $J_K = 3.55t$ they become hybridized. The change of the Fermi

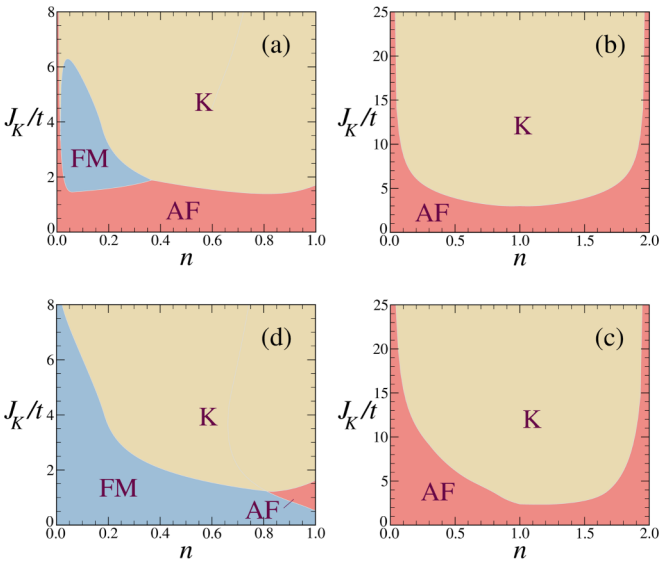

FIG. 4. (Color online) Ground state phase diagram (without phase coexistence) of the KLM on a square lattice for (a) $t' = 0$ and $J = 0.01t$, (b) $t' = 0$ and $J = 0.5t$, (c) $t' = 0.8t$ and $J = 0.5t$, and (d) $t' = 0$ and $J = -0.01t$.

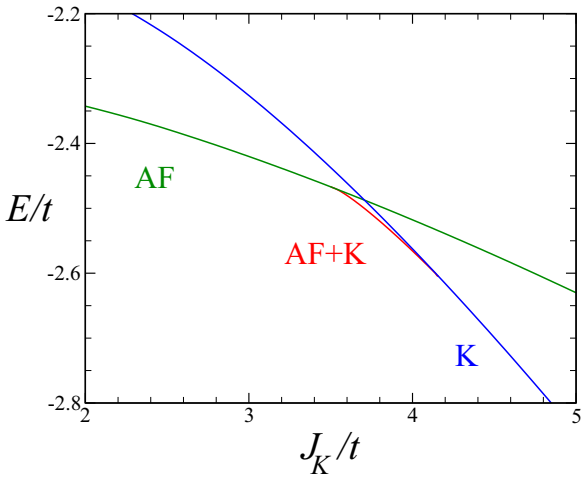

FIG. 5. (Color online) Comparison of the internal energies of the competing phases for $n = 0.8$, $t' = 0.8t$, and $J = 0.5t$.

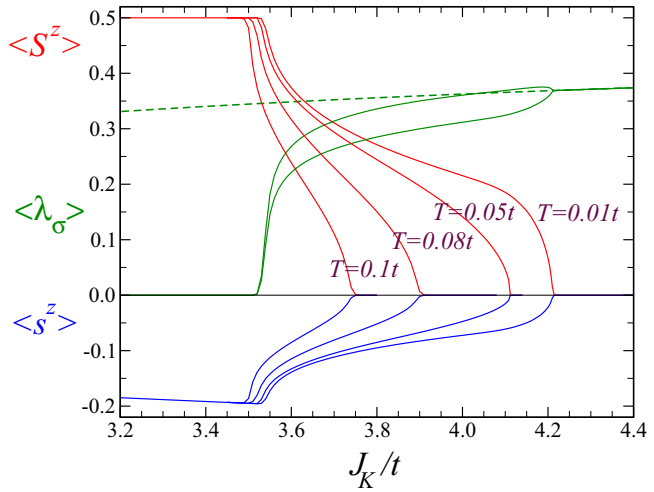

FIG. 6. (Color online) Magnetizations $\langle S_i^z \rangle$ (red) and $\langle s_i^z \rangle$ (blue) as a function of J_K/t for $n = 0.8$, $t' = 0.8t$, and $J = 0.5t$, for different values of T. The averages $\langle \lambda_{i\sigma} \rangle$ (green) are also shown for $T = 0.01t$ (the dashed line corresponds to the pure K solution).

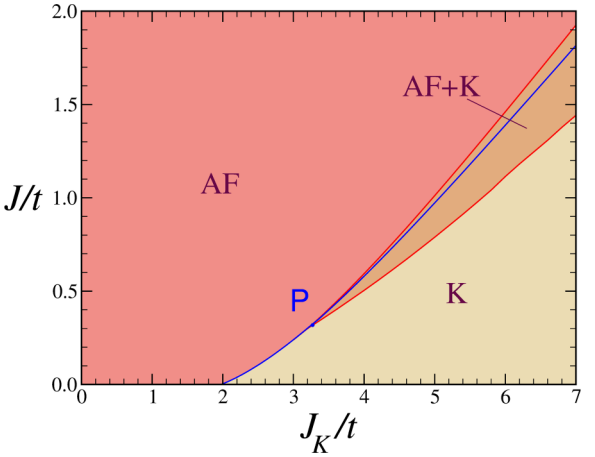

FIG. 8. (Color online) Diagram $J \times J_K$ for $n = 0.8$ and $t' = 0.4t$. The boundary between the underlying pure phases K and AF is indicated by the blue line. The mixed AF + K phase develops around this line on the right of point P.

surface at the AF/AF + K boundary is smooth, and a slight increase of the Fermi volume signalizes the contribution of the f electrons.

Both parameters t' and J (>0) favor antiferromagnetism, and finite values of t' and J are required to produce a region of coexistence AF + K. This is illustrated in Fig. 8 through the diagram $J \times J_K$ for $n = 0.8$ and $t' = 0.4t$. Within numerical precision, the region AF + K seems to collapse at a point P on the boundary AF/K, located at $J_K \approx 3.2t$, $J \approx 0.30t$ for the parameters used in the figure. Below this point one has a direct transition between AF and K phases. For larger values of t' a similar diagram is obtained, where point P is shifted downwards along the AF/K line.

The temperature variation of the averages is shown in Fig. 9. The top panel represents a situation where the ground state corresponds to the mixed AF + K state, where $\langle S_i^z \rangle$ goes to zero at the Néel temperature T_N. For higher temperatures, the

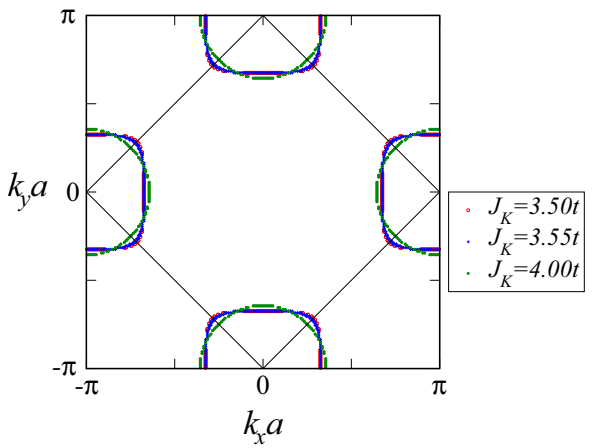

FIG. 7. (Color online) Evolution of the Fermi surface as a function of J_K for the same parameters considered in Fig. 6 with $T = 0.01t$.

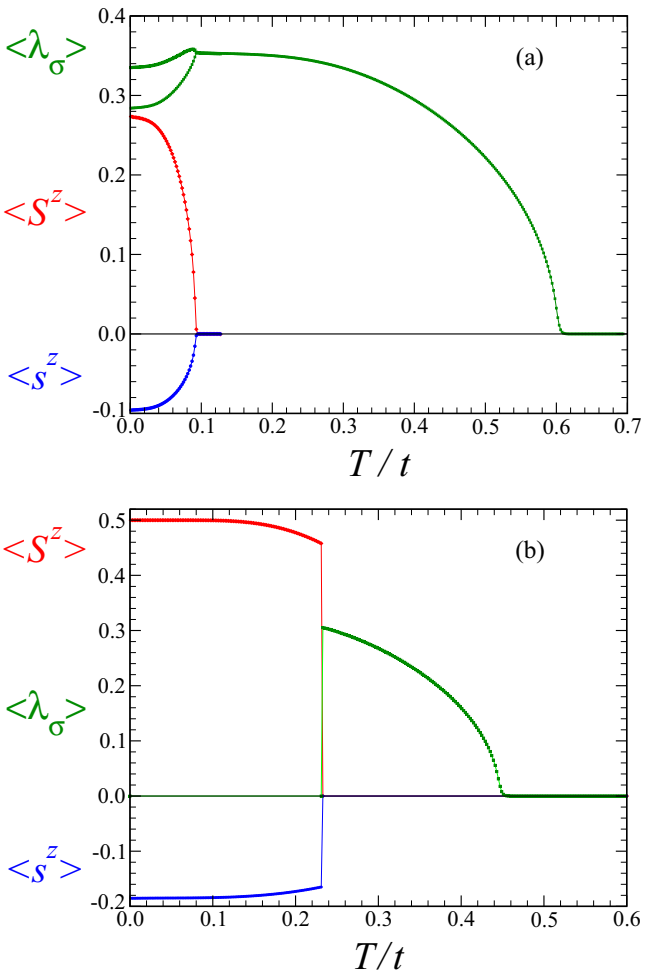

FIG. 9. (Color online) Magnetizations and $\langle \lambda_{i\sigma} \rangle$ as a function of temperature for $n = 0.8$, $t' = 0.8t$, $J = 0.5t$, with (a) $J_K = 3.8t$ and (b) $J_K = 3.2t$.

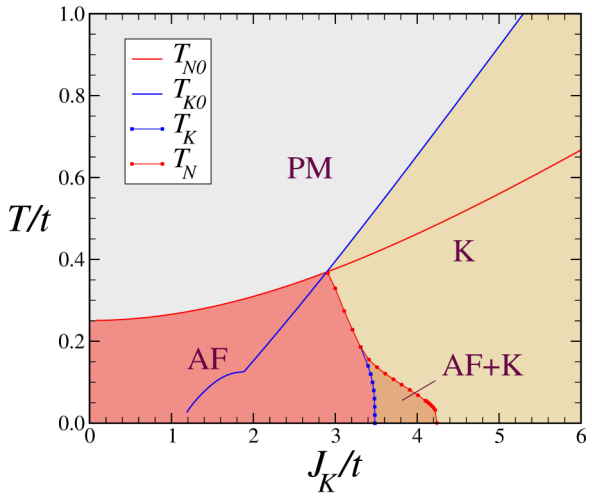

FIG. 10. (Color online) Kondo temperatures T_K and T_{K0} and Néel temperatures T_N and T_{N0} as a function of J_K/t for $n = 0.8$, $t' = 0.8t$, and $J = 0.5t$.

system is in the pure K phase, and eventually the $\langle\lambda\rangle$ value goes to zero at the Kondo temperature T_K. In panel (b), the ground state is the pure AF state, and the system evolves directly to the K phase through a first-order transition.

In Fig. 10, we show the corresponding Doniach diagram, where we plot the curves of T_N and T_K, compared to the corresponding temperatures T_{N0} (in absence of Kondo effect) and T_{K0} (without long-range order). The study of the mixed phase is fundamental to determine the emergence of magnetic order below T_K for values of J_K above the crossing of the curves T_{N0} and T_{K0}. The diagram is similar to the one obtained in Ref. [30] for a simple cubic lattice, where the mixed phase AF + K has been denoted as a spin density wave.

The transition from the K to the PM phase as a function of temperature is a well-known artifact of the method, which demands an appropriate interpretation, as long as no symmetry is broken. This point can be better understood in connection to other approaches, as discussed, e.g., in Ref. [40], where $\langle\lambda\rangle$ is found to decrease monotonically with temperature T. In that case, the Kondo temperature T_K was given by the crossover temperature between the magnetic and Kondo regimes, which can be defined from the minimum of the derivative of $\langle\lambda\rangle$ with respect to T. A similar interpretation may be applied to the transitions between the AF and AF + K phases, or between the FM and FM + K phases described above, as a function of J_K.

When $J \neq 0$, the vanishing of $\langle\lambda\rangle$ at low temperatures with decreasing J_K is expected to occur even in absence of long-range order. This is shown by the curve T_{K0} in Fig. 10 which describes the prolongated boundary between the K and PM phases, which goes to zero at $J_K = 1.1t$. It is a consequence of the short-range correlations driven by J on the K phase, as previously studied in Ref. [21]. The Kondo breakdown is anticipated at low temperature with the emergence of the AF phase (with long-range order), similar to the FM case discussed in Sec. III A.

In the fermionic mean-field approach it implies a topological transition, separating a magnetic phase with a small Fermi surface from a nonmagnetic (K) or magnetic (AF + K) phase, charaterized by a large Fermi surface enhanced by the c-f mixing. In agreement with the discussion in Ref. [4], this Lifshitz transition may coincide or not with the magnetic transition, depending on the existence of the intermediate phase. However, it is important to stress that in our treatment the presence of t' and J (not included in the variational Monte Carlo method of Ref. [4]) is fundamental to produce the coexistence AF + K.

IV. DISCUSSION

From the behavior of the order parameters associated to the FM, AF, and K phases, we have made a quite wide analysis of the phase diagram, being able to identify the regions where the coexistences FM + K and AF + K can be found. The evolution of the phases has been studied as a function of temperature T, electronic concentration n, and the different parameters of the Hamiltonian.

For $t' = 0$ and $J = 0$, the FM phase is present in the phase diagram for $n < 0.586$ and small values of J_K. A coexistence FM + K is realized in a region around the FM-K boundary, which can be divided in the two distinct solutions SSKI and FMK, as shown in Fig. 1. For this case, explicit calculations have also been performed on a simple cubic lattice. The results are qualitatively similar to those shown in Figs. 1 and 3, confirming that the occurrence of a spin-selective Kondo insulator is not restricted to a particular geometry, and suggesting that it may be widespread in heavy-fermion materials.

The presence of t' and J causes a substantial change in the phase diagram, as illustrated in Fig. 4. For moderate positive values of J and t', the AF phase is favored, causing a suppression of the FM phase (and any possible coexistence FM + K). In this case, the coexistence AF + K may be sustained in the neighborhood of the AF/K boundary. Consequently, the magnetic transitions observed in antiferromagnetic heavy-fermion compounds may consist of a direct transition between the pure AF and K states, or an indirect transition passing through the mixed AF + K phase. Such description seems to be consistent with Refs. [4,30], but the nature of the respective AF phase is clearly distinct, which explains the different evolution of the Fermi surfaces.

Here the allowed phases were restricted to the pure FM, AF, K, and their mixed phases. These simple phases can be accounted for by a one- or two-site basis, assuming translational invariance (on each sublattice) and without charge order (CO). We have not found any alternative magnetic solution with $\langle\gamma\rangle \neq 0$ when $\langle\lambda\rangle = 0$. Such solution was reported in Ref. [33], but it requires the tuning of an interpolation parameter (which is absent in our formulation). Other competing phases, such as AF with CO at quarter-filling have not been considered, but they can be addressed by the method in a further work.

The Shastry-Sutherland lattice can be viewed as a square lattice with a four-site basis. We have verified that the results of Ref. [32] for the Shastry-Sutherland lattice remain qualitatively unchanged within the present version of the mean-field decoupling, in particular, the double magnetic transition obtained by varying J_K.

The present results can be verified for the various heavy-fermion compounds within the usual Doniach picture in which

the effect of pressure is mainly governed by the parameter J_K/t. The method can be further explored to describe other competing phases driven by frustration, such as a valence bond solid, spin liquid, charge order, inhomogeneous phases with partial Kondo screening, and the corresponding mixed phases.

ACKNOWLEDGMENTS

B.H.B. acknowledges the support of Brazilian agencies Fundação de Amparo à Pesquisa e Inovação do Estado de Santa Catarina (FAPESC) and Coordenação de Aperfeiçoamento de Pessoal de Nível Superior (CAPES).

[1] S. Doniach, Physica B **91**, 231 (1977).
[2] C. Lacroix and M. Cyrot, Phys. Rev. B **20**, 1969 (1979).
[3] Q. Si and F. Steglich, Science **329**, 1161 (2010).
[4] H. Watanabe and M. Ogata, Phys. Rev. Lett. **99**, 136401 (2007).
[5] L. C. Martin and F. F. Assaad, Phys. Rev. Lett. **101**, 066404 (2008).
[6] S. A. Shaheen and J. S. Schilling, Phys. Rev. B **35**, 6880 (1987).
[7] S. Süllow, M. C. Aronson, B. D. Rainford, and P. Haen, Phys. Rev. Lett. **82**, 2963 (1999).
[8] V. A. Sidorov, E. D. Bauer, N. A. Frederick, J. R. Jeffries, S. Nakatsuji, N. O. Moreno, J. D. Thompson, M. B. Maple, and Z. Fisk, Phys. Rev. B **67**, 224419 (2003).
[9] S. Lausberg, J. Spehling, A. Steppke, A. Jesche, H. Luetkens, A. Amato, C. Baines, C. Krellner, M. Brando, C. Geibel, H.-H. Klauss, and F. Steglich, Phys. Rev. Lett. **109**, 216402 (2012).
[10] A. Steppke, R. Küchler, S. Lausberg, E. Lengyel, L. Steinke, R. Borth, T. Lühmann, C. Krellner, M. Nicklas, C. Geibel, F. Steglich, and M. Brando, Science **339**, 933 (2013).
[11] A. Fernandez-Panella, D. Braithwaite, B. Salce, G. Lapertot, and J. Flouquet, Phys. Rev. B **84**, 134416 (2011).
[12] Q. Si, Physica B **378**, 23 (2006).
[13] P. Coleman and A. Nevidomskyy, J. Low. Temp. Phys. **161**, 182 (2010).
[14] T. Misawa, J. Yoshitake, and Y. Motome, Phys. Rev. Lett. **110**, 246401 (2013).
[15] R. Peters, S. Hoshino, N. Kawakami, J. Otsuki, and Y. Kuramoto, Phys. Rev. B **87**, 165133 (2013).
[16] J. Otsuki, H. Kusunose, and Y. Kuramoto, J. Phys. Soc. Jpn. **78**, 034719 (2009).
[17] Y. Motome, K. Nakamikawa, Y. Yamaji, and M. Udagawa, Phys. Rev. Lett. **105**, 036403 (2010).
[18] C. Lacroix, B. Canals, and M. D. Núñez-Regueiro, Phys. Rev. Lett. **77**, 5126 (1996).
[19] J. R. Iglesias, C. Lacroix, and B. Coqblin, Phys. Rev. B **56**, 11820 (1997).
[20] A. R. Ruppenthal, J. R. Iglesias, and M. A. Gusmão, Phys. Rev. B **60**, 7321 (1999).
[21] B. Coqblin, C. Lacroix, M. A. Gusmão, and J. R. Iglesias, Phys. Rev. B **67**, 064417 (2003).
[22] G. M. Zhang, Y. H. Su, and L. Yu, Phys. Rev. B **83**, 033102 (2011).
[23] A. Hackl and M. Vojta, Phys. Rev. B **77**, 134439 (2008).
[24] N. B. Perkins, J. R. Iglesias, M. D. Núñez-Regueiro, and B. Coqblin, Euro. Phys. Lett. **79**, 57006 (2007).
[25] M. D. Kim, C. K. Kim, and J. Hong, Phys. Rev. B **68**, 174424 (2003).
[26] Y. Liu, G. M. Zhang, and L. Yu, Phys. Rev. B **87**, 134409 (2013).
[27] G. B. Li, G. M. Zhang, and L. Yu, Phys. Rev. B **81**, 094420 (2010).
[28] Z. Z. Li, M. Zhuang, and M. W. Xiao, J. Phys.: Condens. Matter **8**, 7941 (1996).
[29] L. Isaev and I. Vekhter, Phys. Rev. Lett. **110**, 026403 (2013).
[30] T. Senthil, M. Vojta, and S. Sachdev, Phys. Rev. B **69**, 035111 (2004).
[31] G.-M. Zhang and L. Yu, Phys. Rev. B **62**, 76 (2000).
[32] B. H. Bernhard, B. Coqblin, and C. Lacroix, Phys. Rev. B **83**, 214427 (2011).
[33] J. H. Pixley, R. Yu, and Q. Si, Phys. Rev. Lett. **113**, 176402 (2014).
[34] K. S. D. Beach and F. F. Assaad, Phys. Rev. B **77**, 205123 (2008).
[35] S. Viola Kusminskiy, K. S. D. Beach, A. H. Castro Neto, and D. K. Campbell, Phys. Rev. B **77**, 094419 (2008).
[36] R. Peters, N. Kawakami, and T. Pruschke, Phys. Rev. Lett. **108**, 086402 (2012).
[37] H. Tsunetsugu, M. Sigrist, and K. Ueda, Rev. Mod. Phys. **69**, 809 (1997).
[38] J. R. Schrieffer and P. A. Wolff, Phys. Rev. **149**, 491 (1966).
[39] P. Fazekas and E. Müller-Hartmann, Z. Phys. B **85**, 285 (1991).
[40] B. H. Bernhard and C. Lacroix, Phys. Rev. B **60**, 12149 (1999).